

Equation of state of Bose gases beyond the universal regime

Martí Planasdemunt, Jordi Pera,* and Jordi Boronat†

Departament de Física, Universitat Politècnica de Catalunya, Campus Nord B4-B5, 08034 Barcelona, Spain

(Dated: July 26, 2024)

The equation of state of dilute Bose gases, in which the energy only depends on the s -wave scattering length, is rather unknown beyond the universal limit. We have carried out a bunch of diffusion Monte Carlo calculations up to gas parameters of 10^{-2} to explore how the departure from the universality emerges. Using different model potentials, we calculate the energies of the gas in an exact way, within some statistical noise, and report the results as a function of the three relevant scattering parameters: the s -wave scattering length a_0 , the s -wave effective range r_0 , and the p -wave scattering length a_1 . If the effective range is not large we observe universality in terms of a_0 and r_0 up to gas parameters of 10^{-2} . If r_0 grows the regime of universality in these two parameters is reduced and effects of a_1 start to be observed. In the (a_0, r_0) universal regime we propose an analytical law that reproduces fairly well the exact energies.

The experimental realization of the Bose-Einstein condensed state (BEC) [1, 2] has allowed for the study of a dilute Bose gas whose main properties were predicted theoretically many years ago. The high tunability of the interaction strength in these systems offers a unique platform to gain accurate insight on their properties. However, this intriguing feature cannot be carried out as far as theory would like due to the metastability of the dilute BEC in the laboratories [3]. Three-body losses frequently hinder the achievement of large densities n and universality in terms of the gas parameter $x = na_0^3$, with a_0 the s -wave scattering length, is what is normally observed. Nevertheless, we already know of experimental results that go beyond universality: the Fermi polaron in two dimensions [4, 5], dilute Bose-Bose liquid drops [6, 7], and dipolar gases [8, 9].

The first terms of the equation of state of Bose gases were calculated long time ago and proved to be dependent only on the gas parameter,

$$\frac{E_u}{N} = c_{MF} x + c_{LHY} x^{3/2} + c_{WU} x^2 \ln x, \quad (1)$$

with the energy in unities of $\hbar^2/(2ma_0^2)$. The universal constants in Eq. (1) are

$$c_{MF} = 4\pi, \quad (2)$$

$$c_{LHY} = \frac{512\sqrt{\pi}}{15}, \quad (3)$$

$$c_{WU} = \frac{32\pi(4\pi - 3\sqrt{3})}{3}. \quad (4)$$

The first term in Eq. (1) is the mean-field or Hartree-Fock term [10]. The second one was first calculated by Lee, Huang, and Yang [11] and incorporates quantum fluctuations at the lowest order, and finally the last one was obtained by Wu [12]. The LHY and WU terms were first derived by a hard-sphere interaction and, later on, it was proved that they are also valid for repulsive potentials with the same s -wave scattering length [13–16]. Beyond E_u/N (1), the energy of the Bose gas is no more a universal expression depending only on the s -wave scattering length of the potential. Hugenholtz and Pines [17] proposed a continuation of the series (1) in the

form

$$\frac{E}{N} = \frac{E_u}{N} + d_1 x^2 + d_2 x^{5/2} \ln x + \dots, \quad (5)$$

with new coefficients d_i which must depend on the shape of the interatomic potential. These parameters are expected to be related to scattering parameters corresponding to a larger momentum transfer, essentially the s -wave effective range r_0 and the p -wave scattering length a_1 , and also to three-body s -wave contributions [18–21]. This perturbative series for a dilute Fermi gas is well settled up to third order of the gas parameter, the terms beyond the universal regime being known, some of them with analytic expressions and the rest with integrals that are numerically estimated [22, 23]. In this expansion for fermions, the analytic terms depend explicitly on r_0 and a_1 . The knowledge of the nonuniversal terms for the equation of state of a Bose gas is very reduced up to now due to difficulties in the calculation of the required diagrams. The most recent attempt to continue the perturbative series was carried out by Braaten [18, 19]. In this work, an expression beyond the LHY term is proposed with terms that correspond to three-body contributions and another one that depends on r_0 . The weight of the three-body term was determined by a fitting procedure to diffusion Monte Carlo (DMC) results available at that time [24]. As these data was focused to low densities, this parameter was determined with a large uncertainty.

In this paper, we study the equation of state of Bose gases beyond the universal limit using the DMC method [25]. Using different model potentials (Fig. 1), from which we know the low-energy scattering parameters, we explore an extended universality, but now in terms of a_0 , r_0 , and a_1 . Our results show that this hypothesis is approximately correct within a certain domain of r_0 values and maximum density and that results with different interactions, sharing common scattering values, are always closer. We discuss the limitations of the Braaten series [18] to reproduce the DMC results, mainly when the density grows. We propose an empirical form that fits well all the DMC data for a limited set of $|r_0| \lesssim 2$ values and gas parameters up to 1×10^{-2} .

The DMC method solves stochastically the imaginary-time Schrödinger equation providing exact results for the ground-state energy and other properties of the system, within some

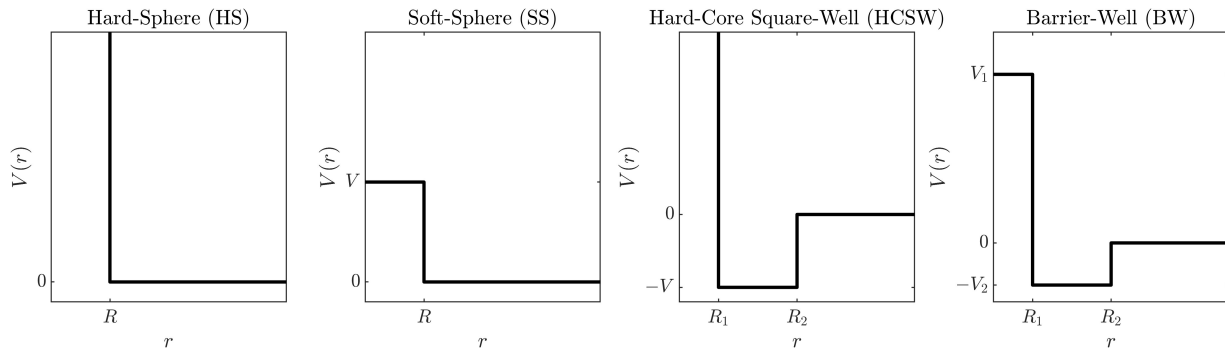


Figure 1. Model potentials used in the DMC calculations.

statistical noise [25]. To reduce the variance one introduces a trial wave function that acts as importance sampling, leading the sampling to regions where the exact wave function is expected to be large and importantly eliminating divergences when the potential becomes singular. The model that we use is a standard Jastrow wave function $\Psi_J(\mathbf{R}) = \prod_{i < j}^N f(r_{ij})$, with $f(r)$ a two-body correlation function. We build $f(r)$ as the two-body solution, properly symmetrized to account well with the periodic boundary conditions (see specific details in Ref. [26]). The time-step and the average number of configurations (*walkers*) is adjusted to eliminate any systematic bias in the results. It is worth noting that our Green's function is accurate to second order in the time step, reducing in this way the time-step dependence and allowing for the use of larger values which reduce the correlation length. The model potentials used in our simulations are shown in Fig. 1 and their characteristic values are chosen to produce the desired scattering parameters.

Our simulations work with finite numbers of particles, confined in a cubic box of the proper size to get the expected bulk density, and thus it is important to study any finite-size effect. This is particularly important in our case because we need to work with the largest possible accuracy. For a fixed density and interaction, we carry on a set of simulations with increasing number of particles, typically in the range $N = 50-700$. Then, we get the energy in the thermodynamic limit E_0/N using the linear law $E/N = E_0/N + \alpha 1/N$ [26]. The time step and asymptotic population of walkers are chosen to eliminate any significant bias coming from these two technical parameters.

Scattering theory at low energy, and up to momentum transfer k^2 , can be developed using three scattering parameters: the a_0 and a_1 scattering lengths [27],

$$a_l^{2l+1} = \frac{1}{2l+1} \int_0^\infty V(r) r^{l+1} u_l^{(0)}(r) dr, \quad (6)$$

corresponding to $l = 0$ and $l = 1$, respectively, and the s -wave effective range

$$r_0 = \frac{2}{a_0^2} \int_0^\infty \left[(r - a_0)^2 - u_0^{(0)2}(r) \right] dr. \quad (7)$$

In Eqs. (6,7), $V(r)$ is the interaction potential, l is the angular momentum quantum number, and $u_l^{(0)}$ is the reduced radial wave function, solution of the radial two-body Schrödinger equation for that potential, with zero energy and angular momentum l . For the model potentials used in our work, these three parameters are analytically known as a function of the parameters defining the interaction [27]. The inverse problem, that is, to know the potential parameters for a given set of scattering parameters is not trivial due to the complex character of the equations to solve. To this end, we implemented a stochastic search that proved to be very efficient (see Ref. [26]).

In Fig. 2 (left panel), we show the departure from the universal regime plotting the DMC energies using the universal energy (1), with $c_{\text{WU}} = 0$, as a reference. From here on, we do not include the logarithmic Wu contribution because it presents a pathological behavior when x grows, even below the universal limit [24]. We have studied densities from $na^3 = 10^{-4}$ up to 10^{-2} and the potentials shown in Fig. 1. Below 10^{-3} , the differences between the different calculations are tiny and not visible at the scale of the plot. This result agrees with previous estimations obtained using also DMC [24], but now the accuracy is improved by using modern CPU's that allow for a more accurate determination of finite-size effects. Increasing more the density, one can appreciate as the energies spread and, at the larger value analyzed in our work (10^{-2}), the effect of finite-range effects is clear. A first significant finding of our study is that energies appear ordered from low to high values of r_0 . To better analyze a possible universality in the (a, r_0) plane, we show in Fig. 2 (right panel) a zoom in a regime of r_0 values around one. Organized in different colors, we show the energies obtained using different potentials that share a common r_0 value. As one can see, at least in this window of r_0 values, the universality in terms of the two s -wave scattering parameters is clearly observed up to the largest density here explored. However, as we will discuss later on, the range of two-parameters universality is significantly reduced when r_0 becomes larger. The role of the p -wave scattering length in the cases reported in Fig. 2 (right panel) is quantitatively below our error bars, since in the figure we plot energies with the same r_0 but distinct a_1 .

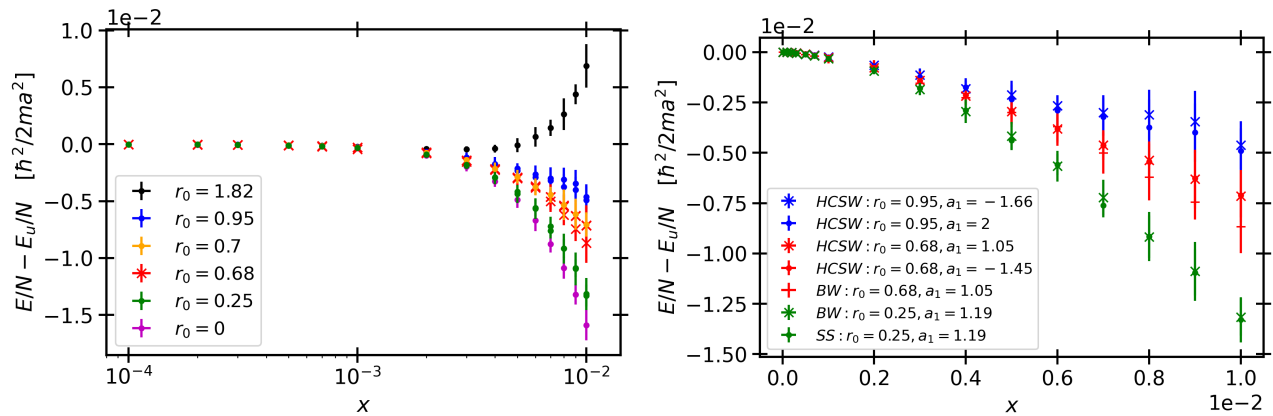


Figure 2. *Left*: DMC energies using different model potentials with a common value of the s -wave effective range r_0 and s -wave scattering length a_0 . The scattering length is used as unite length everywhere. To show the departure from the universal regime, we subtract to the energy per particle the universal term (1). *Right*: DMC energies using different potentials for values of $|r_0| < 2$. Same colors stand for common r_0 values.

Braaten [18] proposed a continuation of the perturbative series beyond the universal regime (1) in the form

$$\frac{E}{N} - \frac{E_u}{N} = 4\pi x \left[\left(c_0 + \frac{4\pi - 3\sqrt{3}}{6\pi} \ln \bar{x} \right) \bar{x} + \left(\frac{8(4\pi - 3\sqrt{3})}{3\pi^2} \ln \bar{x} + c_1 - \frac{16}{15\pi} r_0 \right) \bar{x}^{3/2} \right], \quad (8)$$

with $\bar{x} = 16\pi x$. The parameter c_0 , termed c_E in Ref. [18], is the three-body contact parameter. Braaten *et al.* obtained the value of c_0 by fitting Eq. (8) to DMC energies of Ref. [24], but the scarce data available and their relatively large statistical errors made difficult its estimation. The results found were dependent on the specific interaction, for instance for a HS potential they obtained $c_0 = -0.9 \pm 0.5$ and for a SS one $c_0 = -1.8 \pm 0.8$. It is worth noticing that our results for c_0 are compatible with the estimations in Ref. [18], within the statistical errors.

With the new data obtained in the present work we have repeated the Braaten analysis. We selected energies for effective ranges $|r_0| < 2$ and used both the original model (8) and the one in Eq. (8) but without the logarithmic terms. In both cases, we get statistically compatible fits ($\chi^2/\nu \lesssim 1$) only for gas parameters $x \leq 4 \times 10^{-3}$. With the complete Braaten model (8), we obtained $c_0 = 2.20 \pm 0.06$ and $c_1 = 0.57 \pm 0.16$ whereas, without the logarithmic terms $c_0 = -0.73 \pm 0.06$ and $c_1 = 1.33 \pm 0.15$, the latter showing a slightly better χ^2/ν . The three-body contact parameter c_0 in Eq. (8) keeps a rather constant value $c_0 = 1.2 \pm 0.1$ for energies corresponding to gas parameters $x \leq 7 \times 10^{-4}$. Its absolute value is close to the original Braaten estimation but the sign that we obtain is changed. In Fig. 3, we show the better Braaten equation (8), restricted to the density regime where it is compatible with our results, and the set of DMC points used for the fit (see the table of all the DMC energies in Ref. [26]).

We extended our DMC calculations up to gas parameters

$x = 10^{-2}$, a value which clearly goes beyond the validity of Eq. (8). Inspired by the series expansion proposed by Hugenholtz and Pines [17] (5) we found an empirical equation of state in the form

$$\frac{E}{N} - \frac{E_u}{N} = 4\pi x \left[c_0 \bar{x} + \left(c_1 - \frac{16}{15\pi} r_0 \right) \bar{x}^{3/2} + (c_2 + c_4 r_0) \bar{x}^2 + (c_3 + c_5 r_0) \bar{x}^{5/2} \right], \quad (9)$$

which reproduces well our results. Compared with Eq (8), we notice that we have suppressed the logarithmic terms and increased the order of the expansion up to powers $x^{7/2}$. We verified that we need to go this power in the series if energies up to $x = 1 \times 10^{-2}$ are going to be reproduced. Regarding the logarithmic terms, we did not observe any improvement in the law (9) with their inclusion and thus, we finally removed them. The best set of parameters are reported in Table I, with a value $\chi^2/\nu < 1$. The equations of state for different r_0 values in the range $|r_0| < 2$ are shown, together with the DMC energies, in Fig. 3. As one can appreciate, Eq. (9) is able to reproduce quite accurately the exact energies. For dilute Fermi gases, it is well known that series beyond the universal terms include both the s -wave effective range and the p -wave scattering length a_1 [22, 23]. In the range of r_0 values used for the fit of Eq. (9), we tried to include also the respective values of a_1 that we also known (see Ref. [26]). We used

Table I. Set of optimal parameters of Eq. (9).

c_0	-1.29 ± 0.07
c_1	5.4 ± 0.4
c_2	-9.9 ± 0.9
c_3	6.2 ± 0.6
c_4	2.5 ± 0.08
c_5	-2.33 ± 0.12

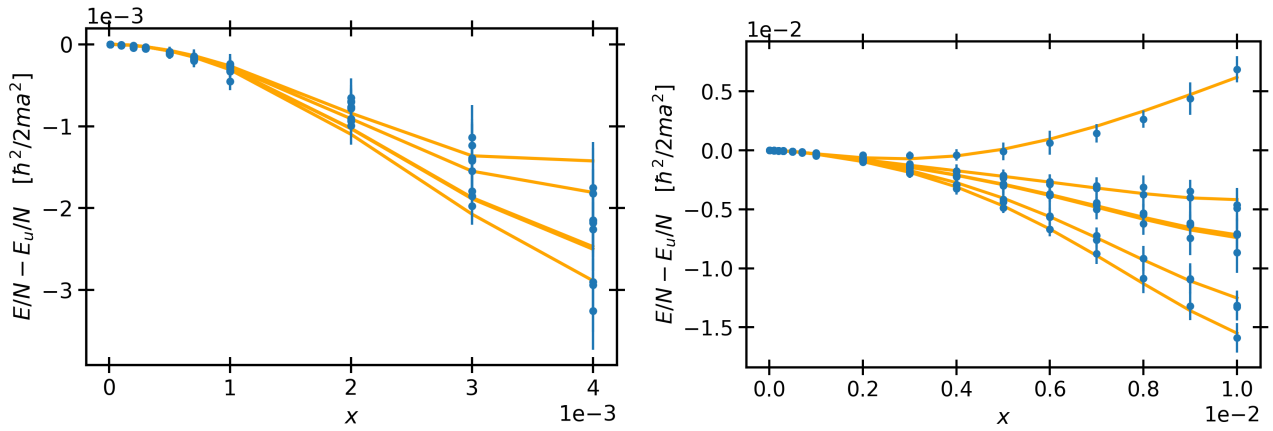


Figure 3. *Left*: Braaten equation of state (8) and the set of DMC energies used for the fit. *Right*: Our proposal for the equation of state (9) and the DMC energies included in the fit. The best parameters are reported in Table I.

different models to include the a_1 values in the equation of state. However, we were not able to discern any effect by introducing these values in the fit. This can also be understood by looking at our results plotted in Fig. 3. There, we show results that have in common r_0 but not a_1 and any meaningful difference is not appreciated.

We carried out more DMC calculations covering larger values of the effective range. However, we were not able to get a reliable equation of state, like Eq. (9), including this extended regime. In Fig. 4, we report the energies obtained for these additional cases, with $r_0 = 19.7$ and $r_0 = -4.96$. For the positive r_0 case, we use two different potentials, HCSW and BW, and the negative case corresponds to a SS model. The first observation on these results is the breaking of universality, in terms of the pair (a, r_0) , for the case of large r_0 at gas parameters $x \gtrsim 3 \times 10^{-3}$. Therefore, the two-parameters universal range depends on the $|r_0|$ value, becoming smaller when it grows. The case of the large r_0 is particularly in-

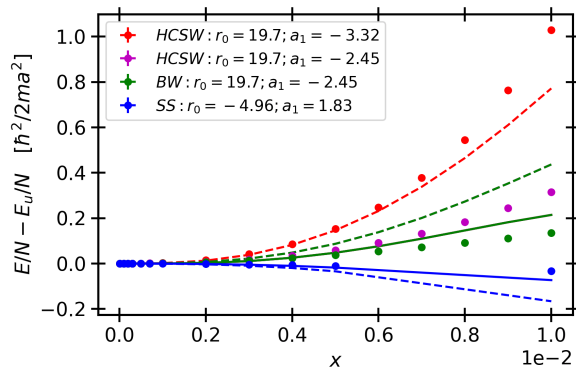


Figure 4. DMC energies for large $|r_0|$ not included in the fit of Eq. (9). The error bars are smaller than the size of the symbols. The solid lines stand for the application of Eq. (9) and the dashed lines incorporate the value of a_1 in the equation of state, as commented in the text.

teresting. In the figure, we show three different calculations with a common r_0 value, two of them sharing the same p -wave scattering length. Even being it not perfect, we can see that the energies when the triplet (a, r_0, a_1) is the same are closer. This indicates that the role of a_1 , which was negligible for small $|r_0|$, becomes significant when the effective range is larger.

We have analyzed if the equation of state (9), fitted to a regime of small effective ranges, is able to reproduce cases out of this domain, even in an approximate form. In Fig. 4, we show with solid lines the predictions of Eq. (9) with the parameters contained in Table I for the two new cases with $r_0 = 19.7$ and $r_0 = -4.96$. The non-universal corrections in both cases are significantly larger than the cases analyzed before (see the different energy scales in Figs. 2 and 4) but still the predictions are rather close to the exact results. Of course, Eq.(9) can not reproduce the dependence on a_1 observed for $r_0 = 19.7$ because this scattering parameter is not included in the model. For the Bose equation of state, there is not any perturbative model which includes a_1 , to the best of our knowledge. Noticeably, in the case of fermions a_1 appears explicitly in the expansion, combined linearly with the effective range. As a first and rather crude attempt, we summed a_1^3 to r_0 in the term $\bar{x}^{3/2}$ of Eq. (9) without any refitting procedure (in a second model we assumed $r_0 + \alpha a_1^3$ with α an adjusting parameter, but the behavior of the energy with a_1 was worse than with a fixed $\alpha = 1$ value). Notice that we add a_1^3 because the phase shift of p -wave scattering is proportional to $k^3 A_1$, A_1 being a volume that is usually written as a_1^3 [27]. The results obtained are shown in Fig. 4 with dashed lines. For the two small $|a_1|$ values, the introduction of a_1 into the equation of state does not improve the results. However, for the largest $|a_1|$ the result is surprisingly accurate. It is also remarkable that the introduction of this scattering parameter reproduces well the ordering of the DMC energies when a_1 changes.

Summarizing, we have explored the equation of state of di-

lute Bose gases by a bunch of DMC calculations of energies, covering a large range of scattering parameters and using different model potentials. The goal of this intensive work was to provide a valuable set of results in order to explore the behavior of the equation of state when universality in terms of the s -wave scattering length ceases. In this regard, this is a continuation of work initiated some years ago in Ref. [24] that allowed to determine the approximated limit of the universality. We have carried out our calculations up to gas parameters $x = 10^{-2}$, quite far of the limit of universality $x < 10^{-3}$. Our results show sizeable deviations of the universal terms, with both positive and negative departures. In the regime $|r_0| < 2$, we clearly observe universality in terms of (a, r_0) , since energies calculated with different model potentials, but sharing these two scattering parameters, are statistically compatible up to $x \simeq 10^{-2}$. In this regime, the equation of state proposed by Braaten [18] reproduces our results but in a smaller density domain, $x < 4 \times 10^{-3}$. We proposed a new equation of state, with terms up to $x^{7/3}$, that reproduces quite accurately the DMC energies up to $x = 10^{-2}$. We used additional energies corresponding to larger values of r_0 to check the validity of our law out of the regime used for the fitting. Contrarily to the energies for small effective range, we observed a sizable effect of the p -wave scattering length. By fixing the set of three parameters (a, r_0, a_1) , we recovered universality, although for not so large values of x . By introducing in the equation of state the a_1 length, we improve our model, mainly for larger values of a_1 . We hope that our DMC calculations [26] can serve to stimulate further theoretical work to improve the equation of state of Bose gases beyond the universal limit. Also, from the experimental side, the estimation of r_0 can serve to effectively improve the study of Bose gases in regimes where the interactions are stronger. Finally, the introduction of the new equation of state in the extended Gross-Pitaevskii formalism [3] can enlarge significantly its domain of applicability.

We acknowledge Joaquim Casulleras for useful discussions to solve the inverse scattering problem. We acknowledge financial support from Ministerio de Ciencia e Innovación MCIN/AEI/10.13039/501100011033 (Spain) under Grant No. PID2020-113565GB-C21 and from AGAUR-Generalitat de Catalunya Grant No. 2021-SGR-01411.

* jordi.pera@upc.edu

† jordi.boronat@upc.edu

- [1] M. H. Anderson, J. R. Ensher, M. R. Matthews, C. E. Wieman, and E. A. Cornell, *Observation of Bose-Einstein Condensation in a Dilute Atomic Vapor*, *Science* **269**, 198 (1995), <https://www.science.org/doi/pdf/10.1126/science.269.5221.198>.
- [2] K. B. Davis, M. O. Mewes, M. R. Andrews, N. J. van Druten, D. S. Durfee, D. M. Kurn, and W. Ketterle, *Bose-Einstein Condensation in a Gas of Sodium Atoms*, *Phys. Rev. Lett.* **75**, 3969 (1995).
- [3] F. Dalfovo, S. Giorgini, L. P. Pitaevskii, and S. Stringari, *Theory of Bose-Einstein condensation in trapped gases*, *Rev. Mod. Phys.* **71**, 463 (1999).
- [4] N. Darkwah Oppong, L. Riegger, O. Bettermann, M. Höfer, J. Levinsen, M. M. Parish, I. Bloch, and S. Fölling, *Observation of Coherent Multiorbital Polarons in a Two-Dimensional Fermi Gas*, *Phys. Rev. Lett.* **122**, 193604 (2019).
- [5] R. Bombín, V. Cikojević, J. Sánchez-Baena, and J. Boronat, *Finite-range effects in the two-dimensional repulsive Fermi polaron*, *Phys. Rev. A* **103**, L041302 (2021).
- [6] C. R. Cabrera, L. Tanzi, J. Sanz, B. Naylor, P. Thomas, P. Cheiney, and L. Tarruell, *Quantum liquid droplets in a mixture of Bose-Einstein condensates*, *Science* **359**, 301 (2018), <https://www.science.org/doi/pdf/10.1126/science.aao5686>.
- [7] V. Cikojevic, L. V. Markic, and J. Boronat, *Finite-range effects in ultradilute quantum drops*, *New Journal of Physics* **22**, 053045 (2020).
- [8] F. Böttcher, M. Wenzel, J.-N. Schmidt, M. Guo, T. Langen, I. Ferrier-Barbut, T. Pfau, R. Bombín, J. Sánchez-Baena, J. Boronat, and F. Mazzanti, *Dilute dipolar quantum droplets beyond the extended Gross-Pitaevskii equation*, *Phys. Rev. Res.* **1**, 033088 (2019).
- [9] R. Bombín, V. Cikojević, F. Mazzanti, and J. Boronat, *Quantum-Monte-Carlo-based functional for dysprosium dipolar systems*, *Phys. Rev. A* **109**, 033312 (2024).
- [10] N. N. Bogoliubov, *On the theory of superfluidity*, *J. Phys. (USSR)* **11**, 23 (1947).
- [11] T. D. Lee, K. Huang, and C. N. Yang, *Eigenvalues and Eigenfunctions of a Bose System of Hard Spheres and Its Low-Temperature Properties*, *Phys. Rev.* **106**, 1135 (1957).
- [12] T. T. Wu, *Ground State of a Bose System of Hard Spheres*, *Phys. Rev.* **115**, 1390 (1959).
- [13] K. A. Brueckner and K. Sawada, *Bose-Einstein Gas with Repulsive Interactions: General Theory*, *Phys. Rev.* **106**, 1117 (1957).
- [14] K. A. Brueckner and K. Sawada, *Bose-Einstein Gas with Repulsive Interactions: Hard Spheres at High Density*, *Phys. Rev.* **106**, 1128 (1957).
- [15] S. Beliaev, *Energy spectrum of a non-ideal Bose gas*, *Sov. Phys. JETP* **7**, 299 (1958).
- [16] E. H. Lieb, *Simplified Approach to the Ground-State Energy of an Imperfect Bose Gas*, *Phys. Rev.* **130**, 2518 (1963).
- [17] N. M. Hugenholtz and D. Pines, *Ground-State Energy and Excitation Spectrum of a System of Interacting Bosons*, *Phys. Rev.* **116**, 489 (1959).
- [18] E. Braaten, H.-W. Hammer, and S. Hermans, *Nonuniversal effects in the homogeneous Bose gas*, *Phys. Rev. A* **63**, 063609 (2001).
- [19] E. Braaten and H.-W. Hammer, *Universality in few-body systems with large scattering length*, *Physics Reports* **428**, 259 (2006).
- [20] E. Braaten and A. Nieto, *Renormalization effects in a dilute Bose gas*, *Phys. Rev. B* **55**, 8090 (1997).
- [21] H.-W. Hammer and R. Furnstahl, *Effective field theory for dilute Fermi systems*, *Nuclear Physics A* **678**, 277 (2000).
- [22] R. Bishop, *Ground-state energy of a dilute fermi gas*, *Annals of Physics* **77**, 106 (1973).
- [23] J. Pera, J. Casulleras, and J. Boronat, *Beyond universality in repulsive SU(N) Fermi gases* (2024), arXiv:2206.06932, accepted for publication in *Scipost Phys. [cond-mat.quant-gas]*.
- [24] S. Giorgini, J. Boronat, and J. Casulleras, *Ground state of a homogeneous Bose gas: A diffusion Monte Carlo calculation*, *Phys. Rev. A* **60**, 5129 (1999).
- [25] J. Boronat and J. Casulleras, *Monte Carlo analysis of an interatomic potential for He*, *Phys. Rev. B* **49**, 8920 (1994).

[26] See Supplemental material, .

[27] J. Pera and J. Boronat, *Low-energy scattering parameters: A theoretical derivation of the effective range and scattering*

length for arbitrary angular momentum, *American Journal of Physics* **91**, 90 (2023).

Supplemental Material for “Equation of state of Bose gases beyond the universal regime”

S1. TRIAL WAVE FUNCTIONS

The DMC algorithm uses a trial or guiding wave function for importance sampling. We use a Jastrow model,

$$\Psi_T(\mathbf{R}) = F_J(\mathbf{R})\Phi(\mathbf{R}). \quad (\text{S1})$$

The one-body term $\Phi(\mathbf{R})$, takes care of the symmetry or antisymmetry of the trial wave function, that is, if particles are bosons or fermions, respectively, as well as other global properties of the system. For a bulk Bose system one just takes $\Phi(\mathbf{R}) = 1$. The second term is the product of two-body correlation functions $f(r_{ij})$ for all pairs $i, j = 1, \dots, N$ in the system,

$$F_J(\mathbf{R}) = \prod_{i < j} f(r_{ij}). \quad (\text{S2})$$

For a central potential, the two-body factor $f(r_{ij})$ is solely determined by the distance between the pair of particles. In this work, we use as a Jastrow factor the exact solution of the two-body problem. In the following, we discuss the explicit forms of $f(r)$ for the different model potentials used in our study.

As our simulations are intended for a bulk system, that we model using periodic boundary conditions, we need to specify the function $f(r)$ for any interparticle distance $r \leq L/2$. We tried two different options: i) match the two-body solution with a smooth function (exponential) going to a constant at the end of that distance, and (ii) to use in all the domain the two-body solution, properly symmetrized. We used both methods and obtained fully compatible results. In the following, we describe the second method, which is easier to build.

We impose that the two-body correlation function $f(r)$ satisfies

$$f(L/2) = 1, \quad f'(L/2) = 0. \quad (\text{S3})$$

For practical reasons, the wave function $\mathcal{R}(r)$ needs to be understood as an exponential, that means $\mathcal{R}(r) = e^{v(r)}$. Its derivative, in terms of $v(r)$ is $\mathcal{R}'(r) = v'(r)e^{v(r)}$. Then, the previous conditions for $v(r)$, but already for the two-body correlation $f(r) = e^{\hat{v}(r)}$ result in

$$e^{\hat{v}(L/2)} = 1 \rightarrow \hat{v}(L/2) = 0, \quad (\text{S4})$$

$$\hat{v}'(L/2)e^{\hat{v}(L/2)} = 0 \rightarrow \hat{v}'(L/2) = 0. \quad (\text{S5})$$

A solution for these two conditions is

$$\hat{v}(r) = v(r) + v(L - r) - 2v(L/2). \quad (\text{S6})$$

Actually, this is a general transformation for any function $v(r)$ to a function $\hat{v}(r)$ that is symmetric with respect to $r = L/2$ in the dominion $0 < r < L$. Its first and second derivatives are

$$\hat{v}'(r) = v'(r) - v'(L - r), \quad (\text{S7})$$

$$\hat{v}''(r) = v''(r) + v''(L - r). \quad (\text{S8})$$

One may verify that, apart from the symmetry, the latter satisfies (S4) and (S5):

$$\hat{v}(L/2) = v(L/2) + v(L - L/2) - 2v(L/2) = 0, \quad (\text{S9})$$

$$\hat{v}'(L/2) = v'(L/2) - v'(L - L/2) = 0. \quad (\text{S10})$$

In the following, we report the detailed solution for each tested potential.

Hard-core square-well (HCSW) To find the solution $f(r)$, the starting point is the two-body solution $\mathcal{R}(r)$. In the case of the HCSW interaction potential, that is

$$\mathcal{R}(r) = \begin{cases} 0 & 0 \leq r < R_1 \\ \frac{A}{r} \sin[k_1(r - R_1)] & R_1 \leq r < R_2 \\ \frac{B}{r} \sin[k_2(r - \delta)] & r \geq R_2 \end{cases} \quad (\text{S11})$$

In terms of $v(r) = \ln \mathcal{R}(r)$,

$$v(r) = \begin{cases} -\infty & 0 \leq r < R_1 \\ \ln \frac{A}{r} \sin[k_1(r - R_1)] & R_1 \leq r < R_2 \\ \ln \frac{B}{r} \sin[k_2(r - \delta)] & r \geq R_2 \end{cases} \quad (\text{S12})$$

The parameters A , B , δ and k_2 are such that verify the boundary conditions of both the function and its derivative. The resulting equations are solved for δ and k_2 , and A , B are left as variational parameters. In fact, only its relation in the form of the quotient A/B is left, as will be seen, since A and B are amplitudes and their absolute value does not affect that $f(L/2) = 1$. One gets

$$A \sin[k_1(R_2 - R_1)] = B \sin[k_2(R_2 - \delta)] \quad (\text{S13})$$

$$A k_1 \cos[k_1(R_2 - R_1)] = B k_2 \cos[k_2(R_2 - \delta)] \quad (\text{S14})$$

The resolution follows isolating δ from (S13),

$$\delta = R_2 - \frac{1}{k_2} \left\{ \arcsin \left(\frac{A}{B} \sin[k_1(R_2 - R_1)] \right) \right\}. \quad (\text{S15})$$

Then, dividing (S13)/(S14), the transcendental equation for k_2 is obtained

$$\frac{\tan[k_1(R_2 - R_1)]}{k_1} = \frac{\tan[k_2(R_2 - \delta)]}{k_2}, \quad (\text{S16})$$

since $k_1(k_2) = \sqrt{V_1 + k_2^2}$ and $\delta = \delta(k_2)$ in (S15) (where the dependence on A/B emerges). Defining $u = k_2$, the latter is transformed into the zero of the function

$$f(u) = \frac{\tan[k_1(u)(R_2 - R_1)]}{k_1(u)} - \frac{\tan[u(R_2 - \delta(u))]}{u}, \quad (\text{S17})$$

which can be calculated using the Newton-Raphson method, using that its derivative is

$$f'(u) = \frac{k_1'(u)(R_2 - R_1)}{k_1(u) \cos^2[k_1(u)(R_2 - R_1)]} - \frac{k_1'(u) \tan[k_1(u)(R_2 - R_1)]}{k_1(u)^2} - \frac{R_2 - \delta(u) - u\delta'(u)}{u \cos^2[u(R_2 - \delta(u))]} + \frac{\tan[u(R_2 - \delta(u))]}{u^2}$$

where

$$k_1'(u) = \frac{2u}{2\sqrt{V_1 + u^2}} = \frac{u}{k_1(u)}, \quad (\text{S18})$$

$$\delta'(u) = \frac{\arcsin \left(\frac{A}{B} \sin[k_1(u)(R_2 - R_1)] \right)}{u^2} - \frac{\frac{A}{B} \cos[k_1(u)(R_2 - R_1)] k_1'(u)(R_2 - R_1)}{u \sqrt{1 - \left(\frac{A}{B} \sin[k_1(u)(R_2 - R_1)] \right)^2}}. \quad (\text{S19})$$

Once solved for $u = k_2$, δ is obtained from (S15). Thus, the analytic expressions of $\mathcal{R}(r)$ and $v(r)$ are obtained.

From now on, the notation $v_1(r)$, $v_2(r)$ is employed to refer to the solution $v(r)$ in the region $R_1 \leq r < R_2$ and $r \geq R_2$ respectively. Since $v(r)$ is a piece-wise function, $\hat{v}(r)$ also is. To construct it, (S6) is applied for each region.

$$\hat{v}(r) = \begin{cases} -\infty + v_2(L-r) - 2v_2(L/2) = -\infty & 0 \leq r < R_1 \\ \hat{v}_1(r) = v_1(r) + v_2(L-r) - 2v_2(L/2) & R_1 \leq r < R_2 \\ \hat{v}_2(r) = v_2(r) + v_2(L-r) - 2v_2(L/2) & R_2 \leq r \leq L/2 \end{cases} \quad (\text{S20})$$

Note that the term $v(L-r)$ always corresponds to the expression $v_2(L-r)$, because $L-r > R_2$ for $0 \leq r \leq L/2$ given that $R_2 < L/2$. Also, $v(L/2)$ corresponds to $v_2(L/2)$ for the same reason. The explicit expressions for the new wave functions are

$$\begin{aligned} \hat{v}_1(r) &= \ln \frac{A}{r} \sin[k_1(r - R_1)] + \ln \frac{B}{L-r} \sin[k_2(L-r-\delta)] - 2 \ln \frac{B}{L/2} \sin[k_2(L/2-\delta)] \\ \hat{v}_2(r) &= \ln \frac{B}{r} \sin[k_2(r-\delta)] + \ln \frac{B}{L-r} \sin[k_2(L-r-\delta)] - 2 \ln \frac{B}{L/2} \sin[k_2(L/2-\delta)] \end{aligned}$$

and $f(r) = e^{\hat{v}(r)}$.

Barrier-well (BW) The two-body solution is

$$\mathcal{R}(r) = \begin{cases} \frac{A}{r} \sinh[k_1 r] & 0 \leq r < R_1 \\ \frac{B}{r} \sin[k_2(r-\delta)] & R_1 \leq r < R_2 \\ \frac{C}{r} \sin[k_3(r-\xi)] & r \geq R_2 \end{cases} \quad (\text{S21})$$

where $k_1 = \sqrt{V_1 - k_3^2}$ and $k_2 = \sqrt{V_2 + k_3^2}$. By imposing the right boundary conditions, one gets

$$A \sinh[k_1 R_1] = B \sin[k_2(R_1 - \delta)] \quad (\text{S22})$$

$$A k_1 \cosh[k_1 R_1] = B k_2 \cos[k_2(R_2 - \delta)] \quad (\text{S23})$$

$$B \sin[k_2(R_2 - \delta)] = C \sin[k_3(R_2 - \xi)] \quad (\text{S24})$$

$$B k_2 \cos[k_2(R_2 - \delta)] = C k_3 \cos[k_3(R_2 - \xi)] \quad (\text{S25})$$

This system of equations is solved for C , δ , ξ , and k_3 . Isolating δ from (S22),

$$\delta = R_1 - \frac{1}{k_2} \left\{ \arcsin \left(\frac{A}{B} \sinh[k_1 R_1] \right) \right\} \quad (\text{S26})$$

and combining (S22)/(S23) and (S24)/(S25), the system is reduced to

$$\frac{\tanh[k_1 R_1]}{k_1} = \frac{\tan[k_2(R_1 - \delta)]}{k_2} \quad (\text{S27})$$

$$\frac{\tan[k_2(R_2 - \delta)]}{k_2} = \frac{\tan[k_3(R_2 - \xi)]}{k_3} \quad (\text{S28})$$

Given its form, setting $B = 1$, and leaving A as a variational parameter, conveniently adjusted, the solution for k_3 , ξ is given by the zero of the multivariate function

$$f(k_3, \xi) = \left(\frac{\tanh[k_1 R_1]}{k_1} - \frac{\tan[k_2(R_1 - \delta)]}{k_2}, \frac{\tan[k_2(R_2 - \delta)]}{k_2} - \frac{\tan[k_3(R_2 - \xi)]}{k_3} \right). \quad (\text{S29})$$

Then, $\delta = \delta(k_3)$ is recovered from (S26) and C is determined from (S24),

$$C = \frac{B \sin[k_2(R_2 - \delta)]}{\sin[k_3(R_2 - \xi)]}. \quad (\text{S30})$$

The resulting transcendental equation is solved by means of a multidimensional Newton-Raphson method. However, this time the derivative $f'(k_3, \xi)$ is approximated numerically, due to the complexity of its analytical expression. To explore its solution, $f(k_3, \xi)$ is understood as two surfaces in the k_3 - ξ plane, given by its first and second components. Then, the initial guess and A values are set provided that both surfaces intersect with the plane $z = 0$, meaning the solution exists. From the two-body solution $\mathcal{R}(r) = e^{\hat{v}(r)}$, one only needs to combine it forming

$$\hat{v}(r) = \begin{cases} \hat{v}_1(r) = v_1(r) + v_3(L-r) - 2v_3(L/2) & 0 \leq r < R_1 \\ \hat{v}_2(r) = v_2(r) + v_3(L-r) - 2v_3(L/2) & R_1 \leq r < R_2 \\ \hat{v}_3(r) = v_3(r) + v_3(L-r) - 2v_3(L/2) & R_2 \leq r \leq L/2 \end{cases} \quad (\text{S31})$$

Again, the term $v(L-r)$ and $v(L/2)$ corresponds to expression for $v(r)$ that holds in the region $R_2 \leq r \leq L/2$, since $L-r > R_2$ for $0 \leq r \leq L/2$ given that $R_2 < L/2$. The explicit expressions are

$$\begin{aligned}\hat{v}_1(r) &= \ln \frac{A}{r} \sin[k_1 r] + \ln \frac{C}{L-r} \sin[k_3(L-r-\xi)] - 2 \ln \frac{C}{L/2} \sin[k_3(L/2-\xi)] \\ \hat{v}_2(r) &= \ln \frac{B}{r} \sin[k_2(r-\delta)] + \ln \frac{C}{L-r} \sin[k_3(L-r-\xi)] - 2 \ln \frac{C}{L/2} \sin[k_3(L/2-\xi)] \\ \hat{v}_3(r) &= \ln \frac{C}{r} \sin[k_3(r-\xi)] + \ln \frac{C}{L-r} \sin[k_3(L-r-\xi)] - 2 \ln \frac{C}{L/2} \sin[k_3(L/2-\xi)]\end{aligned}$$

Soft sphere (SS) The two-body solution is readily obtained,

$$\mathcal{R}(r) = \begin{cases} \frac{A}{r} \sinh[k_1 r] & 0 \leq r < R_1 \\ \frac{B}{r} \sin[k_2(r-\delta)] & r > R_1 \end{cases} \quad (\text{S32})$$

where $k_2 = \sqrt{mE}/\hbar$ and $k_1 = \sqrt{mV_1/\hbar^2 - k_2^2}$. Imposing boundary conditions,

$$A \sinh[k_1 R_1] = B \sin[k_2(R_1 - \delta)] \quad (\text{S33})$$

$$A k_1 \cosh[k_1 R_1] = B k_2 \cos[k_2(R_1 - \delta)] \quad (\text{S34})$$

From (S33), δ can be isolated

$$\delta = R_1 - \frac{1}{k_2} \left\{ \arcsin \left(\frac{A}{B} \sinh[k_1 R_1] \right) \right\}. \quad (\text{S35})$$

Then, as in the previous cases, the solution only depends on the ratio A/B , which is left as a variational parameter that will be properly adjusted. Dividing (S33)/(S34), the transcendental equation for k_2 is obtained,

$$\frac{\tanh[k_1 R_1]}{k_1} = \frac{\tan[k_2(R_1 - \delta)]}{k_2}. \quad (\text{S36})$$

Then, defining $u = k_2$, it becomes the zero of the function

$$f(u) = \frac{\tanh[k_1(u) R_1]}{k_1(u)} - \frac{\tan[u(R_1 - \delta(u))]}{u}, \quad (\text{S37})$$

which can be calculated using the Newton-Raphson method, knowing that its derivative is

$$\begin{aligned}f'(u) &= \frac{k_1'(u) R_1}{k_1(u) \cosh^2[k_1(u) R_1]} - \frac{k_1'(u) \tanh[k_1(u) R_1]}{k_1(u)^2} - \\ &\quad - \frac{R_1 - \delta(u) - u \delta'(u)}{u \cos^2[u(R_1 - \delta(u))]} + \frac{\tan[u(R_1 - \delta(u))]}{u^2}\end{aligned}$$

where

$$k_1'(u) = \frac{-2u}{2\sqrt{mV_1/\hbar^2 - u^2}} = -\frac{u}{k_1(u)} \quad (\text{S38})$$

$$\delta'(u) = \frac{\arcsin \left(\frac{A}{B} \sinh[k_1(u) R_1] \right)}{u^2} - \frac{\frac{A}{B} \cosh[k_1(u) R_1] k_1'(u) R_1}{u \sqrt{1 - \left(\frac{A}{B} \sinh[k_1(u) R_1] \right)^2}} \quad (\text{S39})$$

Once solved for $u = k_2$, δ is obtained from (S35). Thus, the analytic expressions of $\mathcal{R}(r)$ and $v(r)$ are known. Then, the expressions for $\hat{v}(r)$ are

$$\hat{v}(r) = \begin{cases} \hat{v}_1(r) = v_1(r) + v_2(L-r) - 2v_2(L/2) & 0 \leq r < R_1 \\ \hat{v}_2(r) = v_2(r) + v_2(L-r) - 2v_2(L/2) & r \geq R_1 \end{cases} \quad (\text{S40})$$

following the same reasoning as with the previous potentials.

S2. SOLUTION OF THE INVERSE PROBLEM

Given an interaction potential $V(r)$, we are interested in its scattering parameters r_0 (s -wave effective range), a_0 (s -wave scattering length) and a_1 (p -wave scattering length). These are given by

$$a_l^{2l+1} = \frac{1}{2l+1} \int_0^\infty V(r) r^{l+1} u_l^{(0)}(r) dr, \quad (\text{S41})$$

$$r_0^{eff} = \frac{2}{a_0^2} \int_0^\infty \left[(r - a_0)^2 - u_0^{(0)2}(r) \right] dr, \quad (\text{S42})$$

where l is the angular momentum quantum number and has been already substituted by $l = 0$ in Eq. (S42). The function $u_l^{(0)}(r)$ is the reduced radial wave function, solution to the radial two-body Schrödinger equation for that potential, with zero energy and angular momentum l . It must verify the boundary condition $u_l^{(0)}(r = 0) = 0$ (the wave function must vanish at the origin) and be properly normalized to behave as $r^{l+1} - a_l^{2l+1} r^{-l}$ when $r \rightarrow \infty$.

Our interest lies in comparing the energy of systems described by different interaction potentials, each of them with its scattering parameters. To do so, one needs to be able to calculate the scattering parameters of the interaction potentials employed. We refer to Ref. [27] for their explicit analytical expressions, which result from solving Eqs. ((S41),(S42)) for each potential. All the interaction potential models employed are simple, piece-wise functions and can be tuned through a small number of parameters. As an example, if the potential model presents a finite barrier, one can obtain different potentials by changing its width (distance) and height (potential). The referred equations explicitly relate the model's parameters with the scattering parameters. Thus, theoretically one can fix n scattering parameters for a potential model that presents n tuning options. This is exactly what we are interested in: to select any value of the scattering parameters and find the exact different potentials that lead to them, to study the dependencies at wish. The problem here lies in the fact that this association leads to a non-trivial system of equations.

As an example, consider the barrier-well potential. This model consists of a finite barrier and a well around it. The number of tuning options is four: barrier length R_1 , well length R_2 , barrier height V_1 and well height V_2 . Then, one could solve a system of equations for up to four scattering parameters. Since we are only interested in three of them, the system of equations is given by: $a_0(R_1, R_2, V_1, V_2)$, $r_0(R_1, R_2, V_1, V_2)$, $a_1(R_1, R_2, V_1, V_2)$. The expressions can be found in [27], by switching k_1, k_2 to ik_1, ik_2 respectively from the well-barrier equations. This can be done because the barrier-well model is the inverse of the well-barrier, meaning the only difference is a change of sign of the potential values, which affects the equations by turning k_1 and k_2 (the square root of the potential values) imaginary. Then, one could attempt to fix a triad a_0, r_0, a_1 and find the values of R_2, V_1 and V_2 that verify the system of equations. It is not possible to isolate analytically the unknowns from the system of equations, so a numerical method is the only way to proceed. A usual approach is the multidimensional Newton-Raphson method. However, only that does not solve the problem in general; previously it is necessary that one: (i) ensures that there exists a solution for the set of parameters fixed and (ii) provides an initial guess for the unknown variables that is close to the solution of the system of equations.

We use a stochastic strategy to explore the scattering equations, by solving the inverse problem. That means, trying different combinations $\{R_1, R_2, V_1, V_2\}$ and calculating the scattering parameters for each set, employing the equations provided. Then, each combination leads to a point in the (a_0, a_1, r_0) space. Repeating this process for random combinations (all of them feasible for that potential model) provides an idea of the images of the scattering parameters. In the stochastic sense, each combination is a choice and provides a triad which is solution of the scattering parameters. Then, the regions with more density of points are those where it is more likely to find a triad solution. Conversely, the regions with no points are not likely reporting a potential based on that model with those scattering parameters. By inspecting the whole picture, one has an idea about what scattering parameters' triads can be obtained, and, through a simple algorithm, recovers the parameters of the potential model that lead to that triad. Finally, those potential parameters serve as the initial condition for the Newton-Raphson method to find triads similar to the one that is obtained by them, up to the desired accuracy.

This strategy has an even major interest in our scope: it allows us to compare the images of the scattering parameters' equations of different potential models (Fig. S1). Thus, it can be extremely useful to find coincident triads for different potential models and, if possible, which are approximately its values. This case corresponds to a region where two points from different potentials are close in distance.

We choose $a_0 = 1$ for all the interaction potentials, such that the distance is in units of a_0 in the DMC calculations. Hence, we are interested in the points contained in the plane $a_0 = 1$. In fact, Fig. S2 shows the points contained in $a_0 \in [1 - \delta, 1 + \delta]$. Recall that due to the stochastic nature of this strategy, it is not possible to obtain any point with $a_0 = 1$ exactly, thus we select those that are sufficiently close such that they serve as an initial condition for the Newton-Raphson method to find a solution with $a_0 = 1$ exactly.

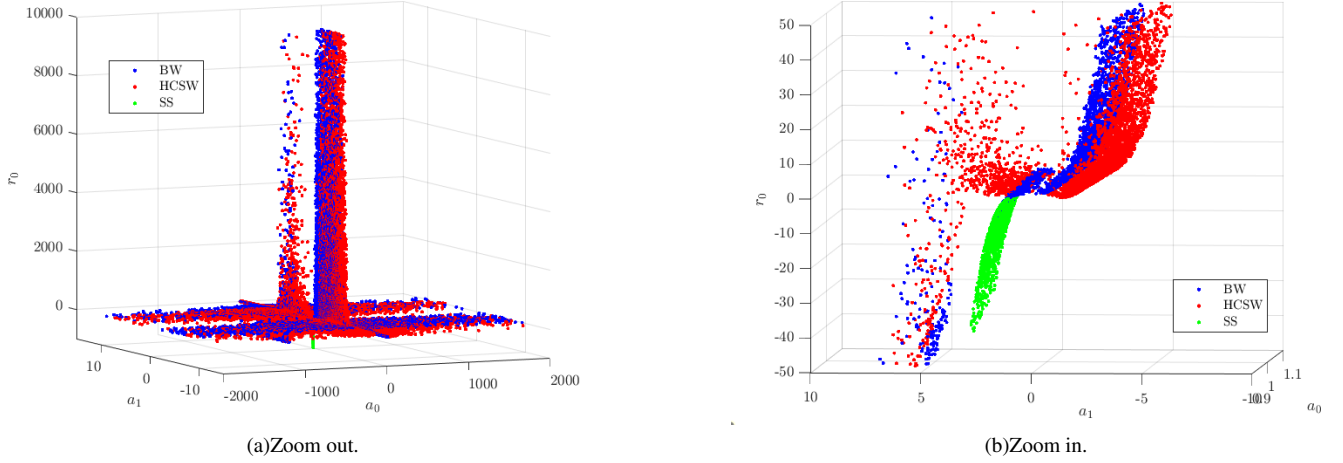


Figure S1. Space of solutions (a_0, a_1, r_0) of the scattering equations for different potentials (see legend) for 10^6 points.

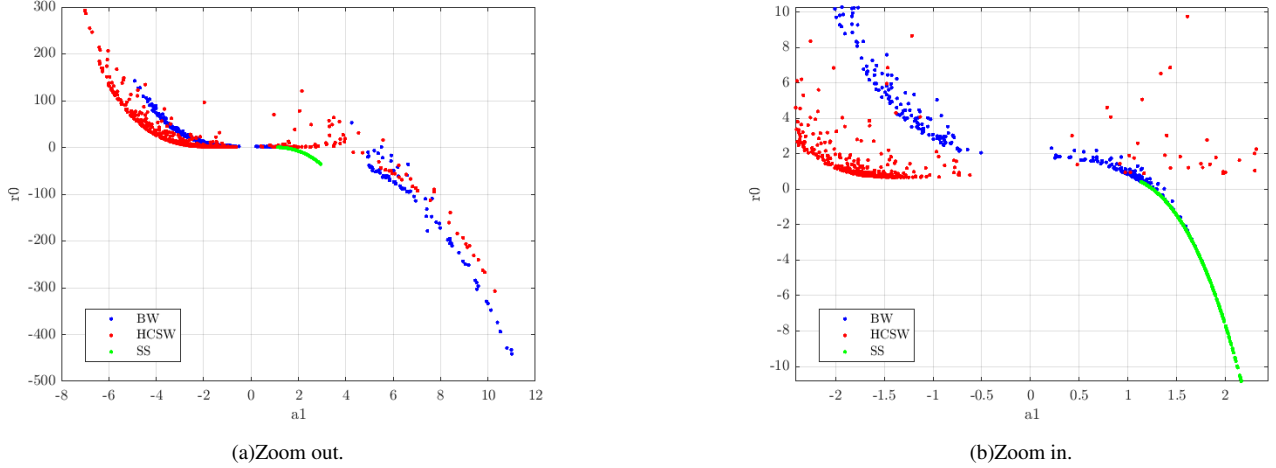


Figure S2. Slice $a_0 \approx 1$ in the space of solutions of the scattering equations for different potentials (see legend) for 10^8 points.

Once a solution triad is found, with its associated potential model parameters, we use them to calculate the scattering parameters differently again (solving the integral forms (S41), (S42)), such that if they coincide the solution is validated. Also, it is checked that a bound state does not appear, the a_0 value of the triad solution being always at the left of the first Feshbach resonance.

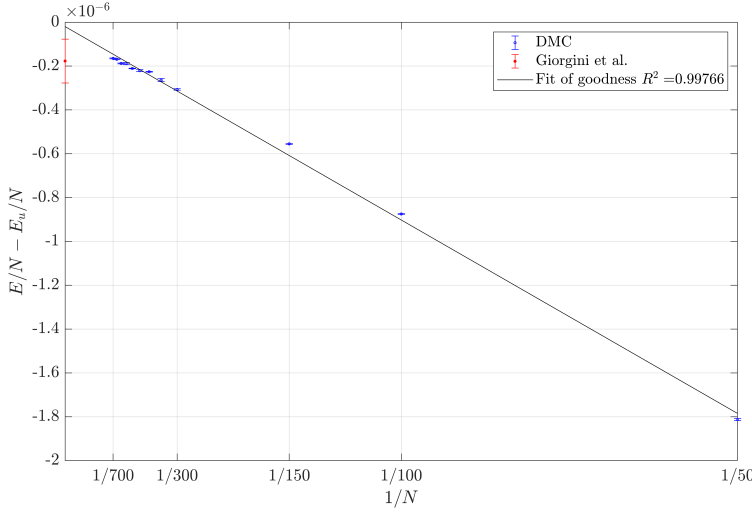
S3. CORRECTION OF FINITE-SIZE EFFECTS IN DMC

A DMC computation is set for a specific number of particles N at a given density n , defining a cubic box of side $L = \sqrt[3]{N/n}$. Obviously, N is limited by the increase of computer time, that grows as $\sim N^2$. We need to estimate finite-size effects because our calculations are intended for a bulk phase in the thermodynamic limit.

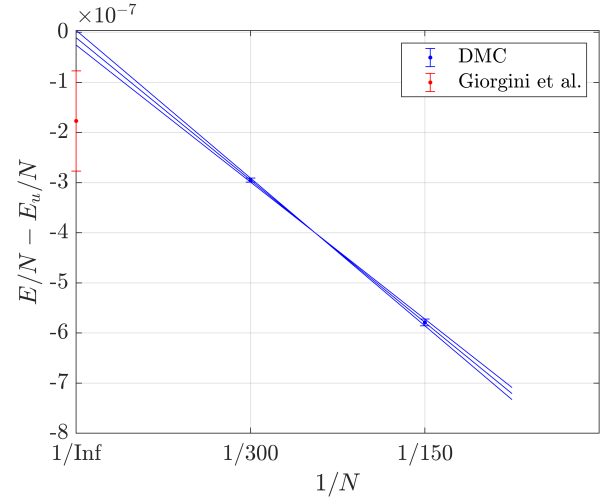
To overcome this issue, we perform several DMC calculations with different numbers of particles and, as a check, we compare our results with E_u/N at a density $na_0^3 = 10^{-5}$ (Fig. S3) where universality holds. A similar analysis is shown in Fig. S4 where E_u/N is no longer valid. Notice that for efficiency reasons in the DMC branching process, the product $E \Delta t$ needs to remain approximately constant, hence the time-step Δt should be reduced when N , and thus E , increases. As an approximation, we deal with this by setting the product $N \Delta t$ constant along DMC calculations with different numbers of particles, at each density and interatomic potential.

We observe that the difference between the energy per particle in the DMC calculation E/N and the universal energy E_u/N is linear with the inverse number of particles $1/N$. At low density, this statement holds in the light of Figure S3(a); while for larger density, Fig. S4(a) the linear law is less accurate. As one can see, at low density the agreement between the extrapolation to $1/N \rightarrow 0$ and the expected result is perfect, improving slightly previous DMC estimations on the same system [24].

Based on the check at low density, all our DMC results consist of calculating the energy with $N = 150$ and $N = 300$, and then extrapolate linearly to the limit $1/N \rightarrow 0$. The errors are safely propagated accordingly. At low density (Fig. S3(b)), this procedure leads to reproducing E_u/N .

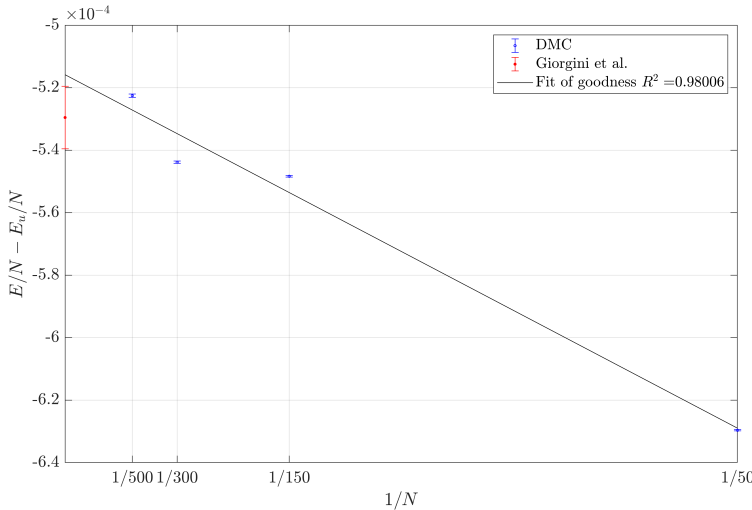


(a) Linear fit to the DMC energies in terms of $1/N$.

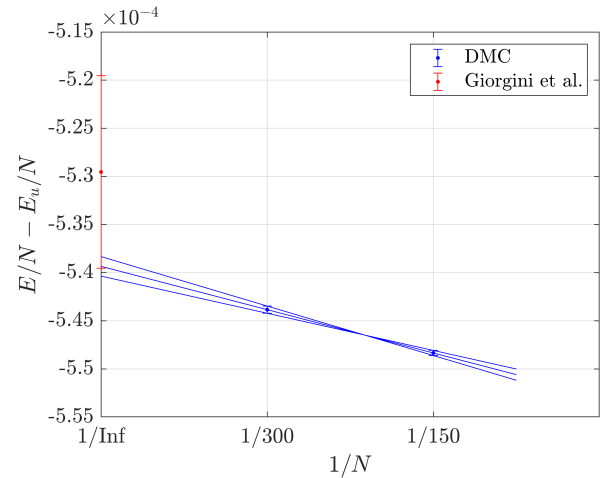


(b) Extrapolation using data obtained with $N = 150$ and 300 .

Figure S3. DMC energies for different numbers of particles interacting through a Hard-Sphere potential at density $na_0^3 = 10^{-5}$.



(a) Linear fit to the DMC energies in terms of $1/N$.



(b) Extrapolation using data obtained with $N = 150$ and 300 .

Figure S4. DMC energies for different numbers of particles interacting through a Soft-Sphere potential (with scattering parameters $r_0 = -4.96$, $a_1 = 1.83$) at density $na^3 = 10^{-3}$.

S4. DMC RESULTS

Model	a_0	r_0	a_1	V_1	V_2	R_1	R_2
SS	1	-4.963717	1.828551	$3.154281E - 2$	-	5	-
SS	1	0.246789895603954	1.192367656777861	0.553699098716986	-	2.25305223642389	-
SS	1	0	1.257306682690198	0.352264068783665	-	2.52455873378522	-
HCSW	1	19.7493	-2.44558	$2.816293678E - 2$	-	2.23871367134203	6.87815732919500
HCSW	1	19.7493	-3.32211	$8.879685093760E - 2$	-	2.65721897814958	5.91964724378216
HCSW	1	0.951316	-1.6636	0.212152394371251	-	1.24099358420681	2.65518281462878
HCSW	1	0.951316	2.00307	$7.4019719854E - 3$	-	1.07208359841336	4.12341010567992
HCSW	1	0.6842384	1.05598013574085	$3.54339300812E - 3$	-	1.01028825874101	3.06371922192216
HCSW	1	0.6842384	-1.4545	$7.14004450115E - 2$	-	1.03334693697237	2.13914846375276
HCSW	1	1.8227872	0.932469981150490	$3.82475925030E - 2$	-	1.29735440984730	4.04020841908368
HCSW	1	0.7	0	$1.01776107899E - 2$	-	1.02287211424451	2.90289035827995
BW	1	19.7493	-2.44558	0.393919355038301	$2.088440731E - 2$	3.73355462692938	7.312800
BW	1	0.6842384	1.05598013574085	0.8005690524	0.101545616787338	2.28829062303712	3.09329071235972
BW	1	1.192368	0.246789895603954	0.55130064452	$5.7315830258E - 3$	2.26041796351839	2.62247347275118

Table II. Parameters of the two-body interaction potentials.

na_0^3	HCSW	HCSW	HCSW	HCSW
	$r_0 = 0.95$ $a_1 = -1.66$	$r_0 = 0.95$ $a_1 = 2.00$	$r_0 = 0.68$ $a_1 = 1.05$	$r_0 = 0.68$ $a_1 = -1.45$
$1.0E - 5$	$1.2633E - 4 \pm 8.7E - 7$	$1.266E - 4 \pm 1.1E - 6$	$1.2695E - 4 \pm 6.5E - 7$	$1.2683E - 4 \pm 8.5E - 7$
$1.0E - 4$	$1.306E - 3 \pm 1.1E - 5$	$1.307E - 3 \pm 1.2E - 5$	$1.306E - 3 \pm 1.2E - 5$	$1.307E - 3 \pm 1.1E - 5$
$2.0E - 4$	$2.667E - 3 \pm 1.7E - 5$	$2.658E - 3 \pm 2.0E - 5$	$2.658E - 3 \pm 2.0E - 5$	$2.654E - 3 \pm 1.7E - 5$
$3.0E - 4$	$4.050E - 3 \pm 3.2E - 5$	$4.040E - 3 \pm 2.4E - 5$	$4.037E - 3 \pm 2.6E - 5$	$4.038E - 3 \pm 2.6E - 5$
$5.0E - 4$	$6.857E - 3 \pm 6.5E - 5$	$6.867E - 3 \pm 6.8E - 5$	$6.862E - 3 \pm 5.8E - 5$	$6.865E - 3 \pm 6.1E - 5$
$7.0E - 4$	$9.773E - 3 \pm 7.0E - 5$	$9.764E - 3 \pm 7.5E - 5$	$9.756E - 3 \pm 6.6E - 5$	$9.758E - 3 \pm 6.2E - 5$
$1.0E - 3$	$1.424E - 2 \pm 1.4E - 4$	$1.422E - 2 \pm 1.2E - 4$	$1.420E - 2 \pm 1.2E - 4$	$1.420E - 2 \pm 1.2E - 4$
$2.0E - 3$	$2.989E - 2 \pm 2.6E - 4$	$2.984E - 2 \pm 2.9E - 4$	$2.976E - 2 \pm 2.1E - 4$	$2.977E - 2 \pm 1.8E - 4$
$3.0E - 3$	$4.650E - 2 \pm 3.0E - 4$	$4.641E - 2 \pm 3.2E - 4$	$4.623E - 2 \pm 4.4E - 4$	$4.622E - 2 \pm 3.5E - 4$
$4.0E - 3$	$6.375E - 2 \pm 3.5E - 4$	$6.382E - 2 \pm 3.3E - 4$	$6.339E - 2 \pm 4.5E - 4$	$6.342E - 2 \pm 4.6E - 4$
$5.0E - 3$	$8.211E - 2 \pm 5.3E - 4$	$8.189E - 2 \pm 6.5E - 4$	$8.127E - 2 \pm 7.4E - 4$	$8.131E - 2 \pm 4.8E - 4$
$6.0E - 3$	$1.0086E - 1 \pm 6.1E - 4$	$1.0062E - 1 \pm 9.4E - 4$	$9.972E - 2 \pm 6.3E - 4$	$9.971E - 2 \pm 6.8E - 4$
$7.0E - 3$	$1.2040E - 1 \pm 7.1E - 4$	$1.202E - 1 \pm 1.1E - 3$	$1.1878E - 1 \pm 6.5E - 4$	$1.188E - 1 \pm 1.1E - 3$
$8.0E - 3$	$1.407E - 1 \pm 1.3E - 3$	$1.4008E - 1 \pm 9.0E - 4$	$1.3844E - 1 \pm 9.5E - 4$	$1.3837E - 1 \pm 7.6E - 4$
$9.0E - 3$	$1.613E - 1 \pm 1.3E - 3$	$1.608E - 1 \pm 1.2E - 3$	$1.5844E - 1 \pm 9.8E - 4$	$1.585E - 1 \pm 1.5E - 3$
$1.0E - 2$	$1.815E - 1 \pm 1.7E - 3$	$1.813E - 1 \pm 1.2E - 3$	$1.790E - 1 \pm 1.2E - 3$	$1.790E - 1 \pm 1.7E - 3$

Table III. DMC energies.

na_0^3	BW	BW	SS	HCSW
	$r_0 = 0.68$ $a_1 = 1.05$	$r_0 = 0.25$ $a_1 = 1.19$	$r_0 = 0.25$ $a_1 = 1.19$	$r_0 = 1.82$ $a_1 = 0.93$
$1.0E-5$	$1.2671E-4 \pm 9.9E-7$	$1.2684E-4 \pm 9.6E-7$	$1.269E-4 \pm 1.1E-6$	$1.257E-4 \pm 1.2E-6$
$1.0E-4$	$1.303E-3 \pm 1.2E-5$	$1.308E-3 \pm 1.1E-5$	$1.307E-3 \pm 1.3E-5$	$1.308E-3 \pm 1.0E-5$
$2.0E-4$	$2.649E-3 \pm 1.7E-5$	$2.656E-3 \pm 2.1E-5$	$2.657E-3 \pm 2.2E-5$	$2.660E-3 \pm 1.4E-5$
$3.0E-4$	$4.032E-3 \pm 3.1E-5$	$4.030E-3 \pm 3.5E-5$	$4.033E-3 \pm 3.7E-5$	$4.045E-3 \pm 4.0E-5$
$5.0E-4$	$6.836E-3 \pm 5.7E-5$	$6.847E-3 \pm 5.9E-5$	$6.847E-3 \pm 6.0E-5$	$6.882E-3 \pm 4.3E-5$
$7.0E-4$	$9.716E-3 \pm 5.5E-5$	$9.731E-3 \pm 6.4E-5$	$9.728E-3 \pm 6.3E-5$	$9.802E-3 \pm 5.7E-5$
$1.0E-3$	$1.403E-2 \pm 1.4E-4$	$1.416E-2 \pm 1.3E-4$	$1.4157E-2 \pm 7.5E-5$	$1.428E-2 \pm 1.1E-4$
$2.0E-3$	$2.985E-2 \pm 1.6E-4$	$2.961E-2 \pm 1.6E-4$	$2.964E-2 \pm 2.5E-4$	$3.014E-2 \pm 2.8E-4$
$3.0E-3$	$4.609E-2 \pm 3.3E-4$	$4.579E-2 \pm 3.6E-4$	$4.585E-2 \pm 4.1E-4$	$4.721E-2 \pm 2.9E-4$
$4.0E-3$	$6.331E-2 \pm 3.5E-4$	$6.263E-2 \pm 3.5E-4$	$6.267E-2 \pm 3.1E-4$	$6.518E-2 \pm 5.3E-4$
$5.0E-3$	$8.122E-2 \pm 7.3E-4$	$8.005E-2 \pm 4.4E-4$	$7.985E-2 \pm 5.8E-4$	$8.413E-2 \pm 7.6E-4$
$6.0E-3$	$9.982E-2 \pm 7.7E-4$	$9.785E-2 \pm 8.2E-4$	$9.794E-2 \pm 9.7E-4$	$1.0416E-1 \pm 9.3E-4$
$7.0E-3$	$1.1839E-1 \pm 9.0E-4$	$1.1618E-1 \pm 6.8E-4$	$1.158E-1 \pm 1.1E-3$	$1.2484E-1 \pm 7.7E-4$
$8.0E-3$	$1.3761E-1 \pm 9.5E-4$	$1.3465E-1 \pm 1.2E-3$	$1.347E-1 \pm 1.3E-3$	$1.4646E-1 \pm 8.8E-4$
$9.0E-3$	$1.5730E-1 \pm 8.9E-4$	$1.5386E-1 \pm 1.5E-3$	$1.538E-1 \pm 1.4E-3$	$1.691E-1 \pm 1.5E-3$
$1.0E-2$	$1.775E-1 \pm 1.6E-3$	$1.730E-1 \pm 1.6E-3$	$1.729E-1 \pm 1.7E-3$	$1.930E-1 \pm 1.9E-3$

Table IV. DMC energies.

na_0^3	HCSW	SS	HCSW	BW
	$r_0 = 0.7$ $a_1 = 0$	$r_0 = 0$ $a_1 = 1.2573$	$r_0 = 19.7493$ $a_1 = -3.32211$	$r_0 = 19.7493$ $a_1 = -2.44558$
$1.0E-5$	$1.268E-4 \pm 1.2E-6$	$1.269E-4 \pm 1.1E-6$	$1.3092E-4 \pm 7.2E-7$	$1.270E-4 \pm 1.1E-6$
$1.0E-4$	$1.306E-3 \pm 1.2E-5$	$1.309E-3 \pm 1.3E-5$	$1.3244E-3 \pm 8.5E-6$	$1.3363E-3 \pm 9.2E-6$
$2.0E-4$	$2.658E-3 \pm 1.4E-5$	$2.642E-3 \pm 2.4E-5$	$2.742E-3 \pm 1.7E-5$	$2.688E-3 \pm 2.2E-5$
$3.0E-4$	$4.038E-3 \pm 3.3E-5$	$4.034E-3 \pm 2.5E-5$	$4.290E-3 \pm 3.8E-5$	$4.154E-3 \pm 2.3E-5$
$5.0E-4$	$6.863E-3 \pm 6.2E-5$	$6.846E-3 \pm 4.0E-5$	$7.569E-3 \pm 4.5E-5$	$7.295E-3 \pm 4.7E-5$
$7.0E-4$	$9.757E-3 \pm 5.6E-5$	$9.734E-3 \pm 7.4E-5$	$1.124E-2 \pm 1.1E-4$	$1.0536E-2 \pm 7.5E-5$
$1.0E-3$	$1.4201E-2 \pm 7.1E-5$	$1.4149E-2 \pm 9.7E-5$	$1.756E-2 \pm 1.5E-4$	$1.5733E-2 \pm 8.7E-5$
$2.0E-3$	$2.978E-2 \pm 2.0E-4$	$2.955E-2 \pm 1.6E-4$	$4.605E-2 \pm 4.1E-4$	$3.595E-2 \pm 3.1E-4$
$3.0E-3$	$4.625E-2 \pm 3.5E-4$	$4.567E-2 \pm 2.6E-4$	$8.922E-2 \pm 6.2E-4$	$6.083E-2 \pm 6.0E-4$
$4.0E-3$	$6.342E-2 \pm 4.7E-4$	$6.231E-2 \pm 3.9E-4$	$1.515E-1 \pm 1.3E-3$	$8.939E-2 \pm 6.0E-4$
$5.0E-3$	$8.136E-2 \pm 5.6E-4$	$7.936E-2 \pm 4.6E-4$	$2.369E-1 \pm 1.7E-3$	$1.2179E-1 \pm 7.6E-4$
$6.0E-3$	$9.977E-2 \pm 8.0E-4$	$9.681E-2 \pm 5.9E-4$	$3.512E-1 \pm 2.3E-3$	$1.568E-1 \pm 1.5E-3$
$7.0E-3$	$1.190E-1 \pm 1.1E-3$	$1.146E-1 \pm 1.0E-3$	$5.017E-1 \pm 2.6E-3$	$1.950E-1 \pm 1.0E-3$
$8.0E-3$	$1.3850E-1 \pm 7.4E-4$	$1.330E-1 \pm 1.2E-3$	$6.886E-1 \pm 3.8E-3$	$2.357E-1 \pm 1.7E-3$
$9.0E-3$	$1.586E-1 \pm 1.3E-3$	$1.5155E-1 \pm 8.5E-4$	$9.284E-1 \pm 6.2E-3$	$2.763E-1 \pm 1.7E-3$
$1.0E-2$	$1.791E-1 \pm 1.3E-3$	$1.703E-1 \pm 1.4E-3$	$1.2158E-0 \pm 7.3E-3$	$3.204E-1 \pm 1.9E-3$

Table V. DMC energies.

na_0^3	HCSW	SS
	$r_0 = 19.7493$ $a_1 = -2.44558$	$r_0 = -4.96$ $a_1 = 1.83$
$1.0E-5$	$1.2717E-4 \pm 9.2E-7$	$1.2712E-4 \pm 6.8E-7$
$1.0E-4$	$1.329E-3 \pm 1.2E-5$	$1.304E-3 \pm 1.1E-5$
$2.0E-4$	$2.724E-3 \pm 2.5E-5$	$2.650E-3 \pm 2.4E-5$
$3.0E-4$	$4.209E-3 \pm 3.8E-5$	$4.025E-3 \pm 3.7E-5$
$5.0E-4$	$7.211E-3 \pm 6.4E-5$	$6.792E-3 \pm 5.4E-5$
$7.0E-4$	$1.0579E-2 \pm 9.5E-5$	$9.622E-3 \pm 6.8E-5$
$1.0E-3$	$1.590E-2 \pm 1.5E-4$	$1.3927E-2 \pm 7.3E-5$
$2.0E-3$	$3.742E-2 \pm 2.9E-4$	$2.855E-2 \pm 2.4E-4$
$3.0E-3$	$6.510E-2 \pm 6.3E-4$	$4.366E-2 \pm 3.1E-4$
$4.0E-3$	$1.0024E-1 \pm 5.4E-4$	$5.898E-2 \pm 5.6E-4$
$5.0E-3$	$1.4327E-1 \pm 7.3E-4$	$7.428E-2 \pm 4.4E-4$
$6.0E-3$	$1.954E-1 \pm 1.6E-3$	-
$7.0E-3$	$2.560E-1 \pm 2.4E-3$	-
$8.0E-3$	$3.272E-1 \pm 1.7E-3$	-
$9.0E-3$	$4.092E-1 \pm 3.5E-3$	-
$1.0E-2$	$5.014E-1 \pm 4.1E-3$	$1.527E-1 \pm 1.1E-3$

Table VI. DMC energies.